

Research Article

Marginal Adaptation and Fracture Resistance of Nanozirconia and Zirconium Dioxide All Ceramic Restoration: An In Vitro Study

Mustafa M. Al-Haddad ¹, Ahmed M. Hamdy ², and Mohamed A. Mokhtar ²

¹Conservative and Esthetic Dentistry Department, Clinician with Practice in Prosthodontics, Faculty of Oral and Dental Medicine, October University for Modern Sciences and Arts (MSA University), 6th of October City 12573, Egypt

²Prosthodontics Department, Faculty of Oral and Dental Medicine, October University for Modern Sciences and Arts (MSA University), 6th of October City 12573, Egypt

Correspondence should be addressed to Mustafa M. Al-Haddad; mostafaelhaddad557@gmail.com

Received 17 December 2024; Revised 10 November 2025; Accepted 13 November 2025

Academic Editor: Murilo Baena Lopes

Copyright © 2026 Mustafa M. Al-Haddad et al. International Journal of Dentistry published by John Wiley & Sons Ltd. This is an open access article under the terms of the Creative Commons Attribution License, which permits use, distribution and reproduction in any medium, provided the original work is properly cited.

Background: The importance of marginal adaptation for long-term success in all-ceramic crowns is highlighted, especially considering the mechanical strength of zirconia, although concerns about its hydrothermal aging and low-temperature degradation (LTD) persist. To overcome these challenges, researchers have developed NANOZR, a nanocomposite that outperforms traditional yttria-stabilized tetragonal zirconia polycrystal (Y-TZP) in terms of strength and resistance to aging degradation in dental applications.

Aim: To evaluate the marginal adaptation and fracture resistance of NANOZR and Y-TZP CAD/CAM restorations before and after thermomechanical aging.

Methodology: The study involved fabricating crowns using two types of zirconia framework materials (NANOZR and Katana Y-TZP) on epoxy resin dies, with and without thermomechanical aging. Standard tooth preparation procedures were followed, including silicone index fabrication, chamfer preparation, and ensuring total occlusal convergence (TOC). The process included reference die fabrication, scanning, framework designing, milling, sintering, veneering, cementation, and aging using a chewing simulator and thermocycling protocol. Marginal adaptation and fracture resistance were evaluated using digital image analysis and a materials testing machine, respectively.

Results: Y-TZP and NANOZR showed marginal gap differences before and after thermomechanical aging, with Y-TZP exhibiting a higher gap postaging. NANOZR demonstrated significantly higher fracture resistance compared to Y-TZP. A negative correlation was observed between fracture resistance and marginal gap, indicating that higher marginal gaps were associated with lower fracture resistance.

Conclusion: NANOZR restorations have superior marginal adaptability compared to Y-TZP restorations following thermocycling.

Keywords: fracture resistance; marginal adaptation; NANOZR; thermomechanical aging; Y-TZP

1. Introduction

Marginal adaptation is considered one of the key factors to determine the long-term success of all-ceramic crowns. Inaccurate marginal fit can lead to different problems, such as microleakage, plaque accumulation, and cement degradation. Moreover, the inadequate marginal fit impairs the

fracture strength of the restoration by creating stress between the restoration and the prepared tooth structure. This will raise the possibility of developing dental carious lesions as well as pulpal and periapical inflammatory response, which can result in undesirable outcomes and the failure of the restoration [1].

Zirconia has been commonly referred to as “ceramic steel” [2] due to its mechanical properties which resemble those of metals, making it the dental ceramic with the highest mechanical properties reported [3, 4]. Yttria-stabilized tetragonal zirconia polycrystals (Y-TZP) are widely used in prosthetic dentistry for the manufacturing of crowns and fixed partial dentures [5]. This is due to the fact that Y-TZP offers several advantages being a dental restorative material, such as excellent dimensional and chemical stability, high mechanical strength and toughness, and a favorable Young’s modulus [6]. On the other hand, one clinical issue that arises is the chipping of the porcelain veneer. Moreover, concerns have been raised regarding the hydrothermal aging of Y-TZP, leading to low-temperature degradation (LTD) [7–9].

Regarding these concerns, researchers have combined ceria-stabilized TZPs (Ce-TZP) with alumina polycrystals (Al_2O_3) to create a nanocomposite known as ceria-stabilized tetragonal zirconia/alumina (NANOZR). In NANOZR, Al_2O_3 nanoparticles are dispersed within Ce-TZP granules [10]. This nanostructured zirconia material has garnered wide application across multiple dental disciplines due to its superior mechanical properties, excellent biocompatibility, and structural stability [11]. A comparison between this material and Y-TZP showed that NANOZR has significantly higher strength and did not show any low-temperature aging degradation (LTAD) after its immersion in aqueous solutions [12, 13]. So, the goal of this in vitro study was to assess the marginal adaptation and fracture resistance of NANOZR and Y-TZP CAD/CAM restorations before and after thermomechanical aging.

2. Materials and Methods

2.1. Specimens Grouping. Twenty-four crowns fabricated on epoxy resin dies from a right mandibular first molar typodont were equally divided into two main groups (A and B) according to the type of zirconia framework material used in the present study ($n = 12$). In Group A, the framework was fabricated from NANOZR (Ce-TZP/ Al_2O_3 ceramic, Kuraray Noritake Dental Inc., Japan), while in Group B, the framework was made of Katana zirconium dioxide (Y-TZP zirconia, Kuraray Noritake Dental Inc., Japan). Fracture resistance was tested only on aged samples (Subgroups A2 and B2) as no preaging control groups were included.

Each group was then subdivided into two subgroups according to the thermomechanical aging. In Subgroups A1 and B1, no thermomechanical aging was performed for NANOZR and Y-TZP, respectively, while in Subgroups A2 and B2, thermomechanical aging was performed for NANOZR and Y-TZP, respectively.

2.2. Master Tooth Preparation. An artificial acrylic mandibular right first molar typodont tooth (El-Banna, Cairo, Egypt) was used as a master tooth for the preparation of all-ceramic crowns according to standard tooth preparation procedures by a single operator [14]. A silicone index (Optosil, Germany) was fabricated prior to tooth preparation to standardize the amount of reduction [15]. A 360° chamfer finish line with a depth of 1.2 mm was prepared, with a uniform occlusal reduction of 2 mm [15] and an occluso-cervical height of 4 mm [16]. The

occlusal reduction and tooth height were standardized to ensure uniformity among all specimens. A custom-made device made from silicone-based material (REPLISIL 22, Dent-E-Con, Gartenstraße, Lonsee, Germany) attached to the surveyor (BEGO, Bremen, Germany) with a diamond bur (Komet Dental, Lemgo, Germany) was used to ensure that the preparation had a total occlusal convergence (TOC) 20° [17]. All sharp margins were rounded [18] and finished 0.5 mm apical to the cemento-enamel junction (CEJ) [19].

2.3. Reference Die Fabrication. Using additional silicon impression material (Imprint II, 3M ESPE, MN, USA), an impression of the prepared master tooth was obtained. To create an epoxy resin die model, the impression was poured into epoxy resin substance (Chema poxy150, CMB chemicals, Egypt). To get 24 epoxy resin dies, this process was performed 24 times. After 24 h to guarantee full setting, epoxy resin dies were taken out of the silicon impression material.

2.4. Reference Die Scanning and Framework Designing. The reference die surfaces were dried and covered with a thin layer of scan reflecting white spray (Identify GmbH, Engen, Germany) to obtain an accurate scan [20]. The reference die was digitally scanned with a 3D optical scanner (NeWay, Open Technologies, Rezzato, Italy) using scanning software (ScanWay, Open Technologies, Rezzato, Italy) to produce 3D virtual die data [21] and obtain an STL (Stereolithography) file [22]. The obtained data from the reference die was then transferred into Exocad software (Exocad GmbH, Julius-Reiber-Straße, Darmstadt, Germany) [21]. According to the manufacturers’ instructions, zirconia frameworks were designed with a uniform wall thickness of 0.3 mm (NANOZR) and 0.5 mm (Y-TZP). The only exception was the area apical to the finish line, where the thickness was increased to 0.5 mm and 0.7 mm, respectively, to accommodate veneering ceramic in accordance with each material’s strength and veneering requirements to ensure optimal support [19]. After setting the zirconia framework margins [23], the virtual luting space was set to $30\ \mu\text{m}$ [24], and the data was saved as an STL file.

2.5. Frameworks Fabrication and Sintering. The data of the completed design was merged and saved [25]. CAD data were sent to the CAM software (Millbox, DGSHAPE, Edition v3.7.3, Roland DG Corp., Hamamatsu, Japan) and then, to a five-axis milling machine (DGSHAPE, DWX 52D, Roland DG Corp., Hamamatsu, Japan). The time required for each framework to be milled was 30 min [24]. Zirconia blank was fixed to the milling machine, and then, the milling process was activated [26]. Cutting burs were replaced for each new zirconia framework [24]. After completion of the milling procedure, zirconia frameworks were separated from the blanks, steam cleaned, and placed in sintering beads (Luoyang Penghao Ceramic Technology, China) prior to being placed in the sintering furnace (YENADENT tegra SPEED 1600, Allée Georges Charpak, Vierzon, France) [21, 24, 26]. According to the manufacturer’s instructions, NANOZR was sintered at 1500°C with a holding time of 2 h, while Y-TZP was sintered at 1450°C with a holding time of 2 h.

2.6. Veneering Procedure. To create an all-ceramic crown, each sintered NANOZR and Y-TZP structure was veneered using feldspathic ceramics using a traditional layering approach. For 10 s, 50 μm Al_2O_3 particles were fired into the surfaces of the NANOZR and Y-TZP frameworks using an airborne-particle abrasion device (P-G 400, Harnisch and Rieth GmbH, Germany) at a pressure of 0.2 MPa. Ten millimeters separated the nozzle from the framework surface vertically. After all frameworks were cleaned with ethanol, they were dried and given a 10 min ultrasonic bath in distilled water [27].

According to the manufacturer's instructions (ZahnfabrikH. Bad Säckingen, Germany), for the dentin layer, VITA VM9 base dentin powder A3 was mixed with modeling liquid to obtain a thin aqueous mixture applied to the dried, cleaned framework whilst ensuring uniform coverage starting from the neck of the crown to obtain the required complete tooth shape. For the enamel layer, several small portions of VITA VM9 enamel EE were applied, beginning from the central third of the crown up to the occlusal surface. To compensate for firing shrinkage, the crown was prepared somewhat larger. The dentin and enamel layers were fired at 900°C using a dental furnace (Programat EP 3000, Ivoclar Vivadent, Schaan, Liechtenstein). Grinding was performed using fine diamond tools under water cooling. Finally, the entire crown was coated with VITA Akzent (Zahnfabrik H. Bad Säckingen, Germany) for glazing and fired at 900°C for 1 min according to the manufacturer's instructions. The finished crowns were then prepared for cementation procedures [27].

2.7. Cementation. The internal surfaces of crowns were grit-blasted for 5 s with 50 μm Al_2O_3 particles using a sandblasting device (Switch Basic Classic, Renfert GmbH, Hilzingen, Germany) under 2 bar pressure [28]. Then, they were put in an ultrasonic cleaner with ethanol for 60 s and cleaned with steam for 60 s. Finally, the inner surfaces of the restorations were silanized with a priming agent (Ceramic Primer II, GC) [29].

For one minute, 40% phosphoric acid (Kuraray America, Inc., New York, NY) was used to etch the replicas made of epoxy resin. Following etching, the surfaces were cleaned with water spray and dried with compressed air that was free of oil [28]. Crowns were checked on their dies, and then luted with dual-cure self-adhesive universal resin cement (G-Cem, GC, Tokyo, Japan) according to the manufacturer instructions [29, 30]. The crowns were seated onto their replicas with finger pressure, and then, 5 kg were applied vertically onto each crown for five minutes by means of a dedicated cementation appliance [29]. Excess cement was removed with a microbrush then each surface of the crown was light-cured for 40 s with a light emitting diode (LED) curing unit (Elipar, 3M ESPE, Seefeld, Germany) [28, 29]. After 1 h of cementation, the crown-die assemblies were stored in 37°C distilled water for at least 24 h until they were subjected to marginal adaptation test [30].

2.8. Thermomechanical Aging. Programmable logic controlled equipment was used to perform mechanical aging; the recently developed four-station multimodal Robota chewing simulator (Model ACH-09075DC-T, AD-Tech., CO., LTD., Germany) operated on a servo-motor while simulating vertical and horizontal movements in conjunction with thermocyclic mode

(chewing simulation test parameters) was integrated with thermocyclic protocol [31]. A weight of 5 kg, which is comparable to 50 N of chewing force, was exerted. The test was repeated 150,000 times to clinically simulate the 12 months chewing condition [32]. The thermocycling protocol consisted of 1200 cycles. Dwell times were 25 s in each water bath (Robota automated thermal cycle; BILGE, Turkey) with a lag time 10 s. The low-temperature point was 5°C, while the high temperature point was 55°C [33, 34].

2.9. Marginal Adaptation Measurements. A measuring stereomicroscope (Nikon Eclips E600, Tokyo, Japan) with a fixed 45x magnification was used for taking photographs of each specimen. The stereomicroscope was connected to an IBM compatible personal computer [35]. To measure and assess the gap width qualitatively, a computerized image analysis system (Image J 1.43U, National Institute of Health, USA) was utilized. Using a holding mechanism that was specifically made for the purpose, specimens were kept in place over the matching dies. Each crown had twenty measurement points, which were dispersed as five fixed landmarks around the cervical circumference for each surface of the crowns, to help identify any marginal gaps [36]. Each measurement location was marked on the prepared tooth to standardize the measurement location before and after aging [35]. After being collected, the data were statistically analyzed. During the gap examination process, a metal device that was specifically created was utilized to help retain the specimen. It was secured by tightening metallic caps on two metallic rods that controlled the upper portion's compressibility [37].

2.10. Fracture Resistance Testing. A computer-controlled materials testing apparatus with a 5 kg load cell held each sample individually, and data were entered using computer software (Instron Bluehill Lite Software) [38]. Screws were tightened to firmly attach samples to the testing machine's lower fixed compartment. In order to achieve uniform stress distribution and minimize the transmission of local force peaks, the fracture test was conducted in the compressive mode of load applied occlusally using a metallic rod with a spherical tip (6 mm in diameter) attached to the upper movable compartment of the testing machine. The rod traveled at a cross-head speed of 1 mm/min with a tin foil sheet in between [38, 39]. The load at failure was manifested by an audible crack and confirmed by a sharp drop in the load-deflection curve recorded using computer software (Bluehill Lite Software, Instron Instruments). The load required to fracture was recorded in Newtons [40].

2.11. Statistical Methods. SPSS version 23.0 was used for data analysis and data management. Numerical data were tested for normality and were described as mean \pm standard deviation (SD). For the marginal gap data, a repeated-measures ANOVA was performed to assess differences in marginal gap values before and after thermomechanical aging. Pair-wise comparisons were adjusted using the Bonferroni correction. In the fracture resistance test, an independent samples *t*-test was used to compare the groups after aging, as each group

TABLE 1: Comparison of marginal gap results (mean values \pm SDs) between both groups before thermomechanical aging.

Variables	Mean \pm SD	Statistics <i>p</i> value
Before thermomechanical aging		
NANOZR group	58.21 \pm 6.81	0.2810 ^{ns}
Y-TZP group	61.99 \pm 9.06	
After thermomechanical aging		
NANOZR group	67.06 \pm 4.24	0.0352*
Y-TZP group	71.68 \pm 5.28	

Note: ns ($p > 0.05$).

Abbreviation: ns, nonsignificant.

*Significant ($p < 0.05$).

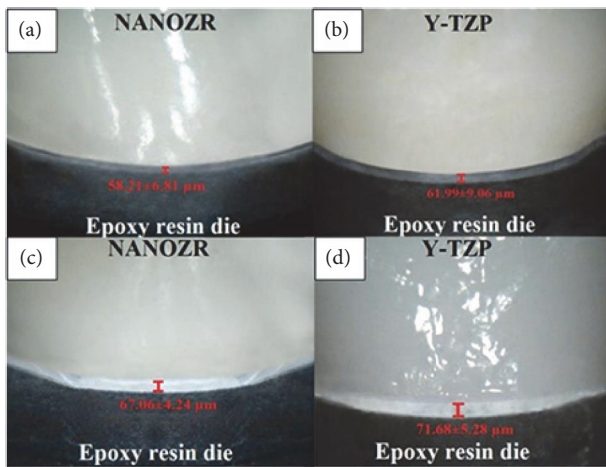


FIGURE 1: Stereomicroscope images for marginal gap of (a) NANOZR and (b) Y-TZP before thermomechanical aging. (c) NANOZR and (d) Y-TZP after thermomechanical aging.

consisted of distinct specimens. The level of significance was set at $p < 0.05$.

3. Results

3.1. Marginal Adaptation. Before thermomechanical aging, it was found that the Y-TZP group showed a statistically nonsignificant marginal gap mean value (61.99 \pm 9.06 μm) than the NANOZR group (58.21 \pm 6.81 μm) at ($p = 0.2810$). After thermomechanical aging, it was found that the Y-TZP group recorded a statistically significant higher marginal gap mean value (71.68 \pm 5.28 μm) than the NANOZR group (67.06 \pm 4.24 μm) at $p = 0.0352$, as shown in Table 1 and Figure 1.

A comparison between the mean values of the marginal gap within each group showed that both groups recorded statistically significant greater marginal gap mean values after thermomechanical aging at $p < 0.05$ (Table 2).

The total effect of material type, regardless of thermomechanical aging, totally there was no significant difference between both groups at $p = 0.0697$ (Table 3).

3.2. Fracture Resistance. It was found that, NANOZR group recorded statistically significant higher fracture resistance mean value (4693.25 \pm 283.75 N) than Y-TZP group

TABLE 2: Descriptive statistics of marginal gap results (mean values \pm SDs) for both groups before and after thermomechanical aging.

Variables	Mean \pm SD	Min.	Max.	95% CI		Statistics <i>p</i> value
				Low	High	
NANOZR group						
Before	58.21 \pm 6.81	45.65	64.86	54.36	62.06	0.002*
After	67.06 \pm 4.24	60.95	74.95	64.66	69.46	
Y-TZP group						
Before	61.99 \pm 9.06	51.55	75.31	56.87	67.12	0.006*
After	71.68 \pm 5.28	61.41	82.84	68.69	74.66	

Note: ns ($p > 0.05$).

Abbreviation: ns, nonsignificant.

*Significant ($p < 0.05$).

TABLE 3: Comparison of total marginal gap results (mean values \pm SDs) between both groups.

Variables	Mean \pm SD	Statistics <i>p</i> value
Material		
NANOZR group	62.63 \pm 5.53	0.0697 ^{ns}
Y-TZP group	66.83 \pm 7.17	

Note: ns ($p > 0.05$).

Abbreviation: ns, nonsignificant.

*Significant ($p < 0.05$).

(2654 \pm 409.5 N) as indicated by student *t*-test ($p = < 0.0001 < 0.05$), as shown in Table 4.

3.3. Correlation Between Fracture Resistance and Marginal Gap. It was found that there was negative (inverse) correlation between fracture resistance and marginal gap as indicated by Pearson linear correlation (correlation coefficient ($r = -0.4829$, $r_2 = 0.2331$, and $p > 0.05$; Figure 2).

4. Discussion

Marginal adaptation represents a key determinant of the long-term clinical success and durability of all-ceramic crowns [41]. Inaccurate marginal fit can lead to a variety of issues, including the buildup of plaque, microleakage, and cement degradation. Because of the stress created between the restoration and the prepared tooth, a poor marginal fit also affects the fracture strength of the restoration itself [42, 43]. As a result, there is an increased chance of caries lesions as well as pulpal and periapical inflammation, which could have negative effects and cause the restoration to fail [1]. The aim of this in vitro study was to evaluate the marginal adaptation of NANOZR and Y-TZP CAD/CAM restorations before and after thermomechanical aging.

In the present study, the parameters related to tooth preparation design, dimensions, and framework fabrication were standardized to ensure consistency between crowns veneered with porcelain and those pressed with ceramic. All crowns were fabricated by a single experienced dental laboratory technician following a unified and standardized protocol. A surveyor was employed to verify that the axial walls of each preparation exhibited a uniform taper consistent with the adjacent

TABLE 4: Descriptive statistics of fracture resistance results (mean values \pm SDs) for both groups after thermomechanical aging.

Variables	Mean \pm SD	Min.	Max.	95% CI		Statistics <i>p</i> value
				Low	High	
Material						
NANOZR group	4693.25 \pm 283.75	4268	5122	4502	4884	<0.0001*
Y-TZP group	2654 \pm 409.5	2089	3473	2379	2929	

Note: ns ($p > 0.05$).

Abbreviation: ns, nonsignificant.

*Significant ($p < 0.05$).

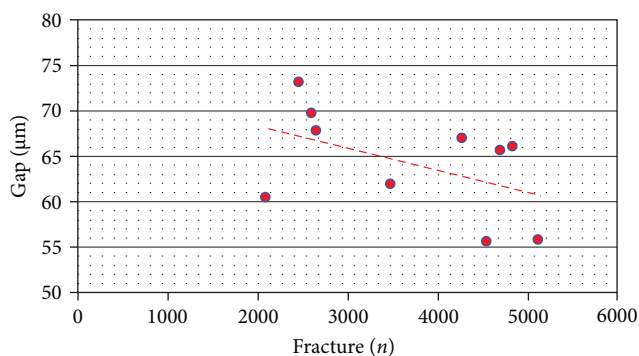


FIGURE 2: Linear chart showing correlation between fracture resistance and marginal gap.

perpendicular bur, as described by El-Dessouky et al. [36]. Finally, a silicone index was utilized to confirm the uniformity and accuracy of tooth reduction.

In the present study, a cement space of 30 μm was used, as has been recommended in the literature for resin cements, but in real practice, this space considerably varies. Numerous factors, including cementation technique, cement type, occlusal pressure used during cementation, preparation angles, laboratory errors, and the lack of cement escape channels on the occlusal surface, have been noted in the literature regarding this difference in cement spacing [44]. The crowns in the current study were luted to their resin dies by means of resin cement, in agreement with Campos et al. [45] and Yüksel and Zaimoğlu [46]. A 5 kg weight was used to keep the crowns in place during the primary cement setting for 5 min by means of a dedicated cementation appliance to ensure a uniform seating pressure in agreement with Zahran et al. [28] and Sadighpour et al. [47].

Theoretically, the restoration needs a luting cement film of 20–40 μm thickness [48]. The cement layer usually requires a space between 25 and 50 μm in agreement with Ferrini et al. [24]. Castillo-Oyagüe et al. [49] defined clinically acceptable values for the marginal gap after cementation to be smaller than 150 μm . Discrepancies of all samples in this study were situated below 120 μm in agreement with Yildiz et al. [50] and Yüksel and Zaimoğlu [46] who agreed that, a marginal gap between 100 and 120 μm appears to be in the range of clinical acceptance.

Three key components must be present in order to simulate aging: (1) oral cavity water, which causes subcritical fracture formation in ceramic materials. (2) Thermal stressing, which

causes dental restorations' mechanical stability to decline. (3) The mechanical force used to replicate the act of chewing. In a similar investigation, the highest load was 100 N, whereas 50 N was utilized to approximate this. But the research indicates that the chewing forces hardly ever go above 50 N [15].

In the current study, the number of thermocycling cycles used were 1200 cycle's (5–55°C), this agree with Choi et al. [33] and Yousry et al. [34], who considered these values the closest to the physiology of the oral cavity. While the number of chewing cycles used in this study was 150,000 cycle's equivalents to 12 months in agreement with Nawafleh et al. [32] and Rosentritt et al. [51], who found that, with a load of 50 N, a total of 750,000 cycles are necessary to simulate 5 clinical years.

Assessing the marginal adaptability of CAD/CAM restorations can be done in a variety of ways. Microphotography, light microscopy, silicone replicas of the fit between the abutment and the restoration, silicon weight and density assessment, virtual 3D analysis using a noncontact scanner and specialized software, and micro-computerized tomographic (micro-CT) technology without an impression of cementation are some methods that can be used to evaluate marginal adaptation (108). In the current investigation, the image was transferred to the computer software using a digital camera that was fastened to the stereomicroscope [52], this was in agreement with De Santi Alvarenga et al. [53], who proved that, measurements obtained using this nondestructive method, were accurate.

Moreover, the advantage of working with a digital camera is that the image can be easily manipulated. Twenty measurement points per crown distributed as four fixed landmarks (buccal, distal, lingual, and mesial) along the cervical circumference for each surface of the crown were recorded in agreement with El-Dessouky et al. [36], who stated that a minimum number of 20–25 measurements per crown were required for in vitro testing.

The current study revealed that, following thermomechanical aging, the marginal gaps measured for NANOZR group (67.06 \pm 4.24 μm) were statistically significantly lower than the Y-TZP group (71.68 \pm 5.28 μm), but both systems demonstrated acceptable marginal discrepancies in vitro below 110 μm , a value defined as clinically acceptable [54]. The difference in marginal adaptation between NANOZR and Y-TZP after aging may be attributed to their distinct microstructural compositions. NANOZR, composed of Ce-TZP/ Al_2O_3 nanocomposite containing 10 mol% ceria-stabilized zirconia and 30 vol% alumina, exhibits an interpenetrating microstructure, in which 10–100 nm Al_2O_3 particles are embedded within ZrO_2

grains and 10 nm ZrO₂ particles are dispersed within Al₂O₃ grains [55]. This unique configuration enhances phase stability and minimizes susceptibility to hydrothermal degradation when compared with Y-TZP, whose yttria-stabilized tetragonal structure is more prone to tetragonal-to-monoclinic phase transformation [7, 56, 57].

Additionally, intragroup analysis showed that both materials had a statistically significant higher marginal gap mean value after thermomechanical aging. The NANOZR group exhibited a marginal gap of $58.21 \pm 6.81 \mu\text{m}$, which increased to $67.06 \pm 4.24 \mu\text{m}$ after thermomechanical aging, representing an approximate 15.2% increase ($p = 0.002$). Similarly, the Y-TZP group recorded a marginal gap of $61.99 \pm 9.06 \mu\text{m}$ that increased to $71.68 \pm 5.28 \mu\text{m}$, corresponding to a 15.6% increase ($p = 0.006$). The comparable percentage increase observed in both groups indicates that thermomechanical aging affects their marginal adaptation to a similar extent, despite differences in their microstructural composition. For NANOZR, the postaging increase may be attributed to its Ce-TZP/Al₂O₃ nanocomposite architecture, which—although resistant to LTD—may experience minor thermal expansion mismatches between the Ce-TZP matrix and Al₂O₃ particles during thermocycling, generating localized micro-stresses at the margins. Conversely, the increase in Y-TZP may be associated with its susceptibility to LTD, in which water penetration and cyclic thermal exposure promote the tetragonal-to-monoclinic phase transformation, resulting in a 3%–5% volumetric expansion and subsequent compressive stresses that distort the margins, as noted by Tanaka et al. [57].

In a SEM study [58], NANOZR was found to be composed of 10 mol% CeO₂ stabilized TZP as a matrix and 30 vol% of Al₂O₃ as a second phase. The average grain size of the NANOZR was 0.49 μm . Its intergranular nanostructure, in which many 10–100 nm-sized Al₂O₃ particles are trapped within the ZrO₂ grains and numerous 10-nm-sized ZrO₂ particles are trapped within the Al₂O₃ grains, is its most notable structural feature [55]. This composite showed excellent phase stability, even after long-term *in vivo* and *in vitro* aging treatments, as remarkable phase transformations were observed for conventional Y-TZP under conditions of aging Tanaka et al. [57].

Moreover, Ban et al. [59] found no change in the contents of NANOZR with aging under various water-based conditions while Y-TZP dramatically changed with autoclaving at 120°C. Additionally, the biaxial flexure strengths of Y-TZP slightly changes with autoclaving, whereas those of NANOZR showed no significant change and was significantly stronger than Y-TZP [14].

Additionally, the melting of porcelain particles caused contraction of the veneering porcelain resulting in compressive forces on the framework. This deformation spread around the whole marginal circumference. El-Dessouky et al. [36] found that CAD/CAM machining of the presintered Y-TZP blocks induced micro-cracks at the zirconia surface, which cannot be completely eliminated by sintering. These micro-cracks serve as stress concentration sites due to the presence of water from the wet veneering porcelain and the high temperature during firing cycles. As a result, the microcracks

continue to grow as water migrates into the zirconia lattice, initiating the tetragonal-to-monoclinic phase transformation that causes a 3%–5% volume increase and compressive stresses within the frameworks. These stresses are believed to be a contributing factor to the marginal distortion that develops during veneering of CAD/CAM frameworks, together with those brought on by the mismatch in the (core-veneer) coefficient of thermal expansion (CTE).

The marginal adaptation of each crown may vary greatly at different locations resulting in an increase in the SD, which is in line with El-Dessouky et al. [36] who found that, the shrinkage of zirconia frameworks and the firing shrinkage of the veneering porcelain may contribute to this fact. The values of SDs reported in the literature ranged between 1.1 and 20 μm while the mean values of the present study were accompanied by SDs between 4.24 and 9.06 μm which are relatively small reflecting consistent results.

Occlusal loading is a significant factor in the mechanical assessment, which was conducted using a universal testing machine to measure the fracture resistance for both zirconia groups. Previous studies have employed a 6 mm steel sphere to test for fracture resistance [39, 60, 61]. The diameter of this indenter was shown to be ideal for molars and premolars because it contacts the functional and nonfunctional cusps in positions close to those found clinically. A wide range of cross head speeds were reported, ranging from 0.5 to 10 mm/min in agreement with Hammad et al. [62]. Therefore, a cross head speed of 1 mm/min was used in this study.

Following thermomechanical aging, the fracture resistance of NANOZR group ($4693.25 \pm 283.75 \text{ N}$) showed statistically higher results than that of Y-TZP group ($2654 \pm 409.5 \text{ N}$) and above the clinically required initial strength (1000 N) for zirconia [63, 64]. The superior results of NANOZR could be explained due to the microstructure with a decrease in the flaw size for both the ZrO₂ and the Al₂O₃ grains associated with the interpenetrated intragranular nanodispersion. Furthermore, several 10–100 nm sized inclusions, which are trapped inside the ZrO₂ and/or Al₂O₃ grains, are believed to have a role in dividing a grain size into finer sized particles by forming subgrain boundaries, this in agree with Ban et al. [12], Sato et al. [13], and Ban et al. [65].

Compared to Y-TZP, NANOZR's fracture surface has a significantly higher monoclinic phase composition. Therefore, the microstructure of NANOZR, or the interpenetrated intragranular nanodispersion, determines how strong it is [13]. It can be interpreted that, the microstructure of NANOZR may be beneficial for the toughening due to the phase transformation and crack bridging, this agree with Ban et al. [12, 65].

Ban [66] demonstrated similar Weibull moduli for fracture strengths of NANOZR and Y-TZP, 2.9 and 3.1, respectively, whereas the characteristic strengths of NANOZR was much higher than that of the Y-TZP, indicating a better reliability against the load-bearing. Ban et al. [12] and Harada et al. [67] reported that there is almost no occurrence of the LTAD seen in Y-TZP, therefore, it is stable enough to be used long-term in the harsh oral environment. Kuroda et al. [68] suggested to remove 1.0–2.0 mm from the abutment tooth in conventional all-ceramic restorations, but with NANOZR, it is possible to

manufacture thin frames of 0.3–0.5 mm for adhesive bridges and single crowns. For this reason, the amount removed from the abutment tooth is reduced, resulting in a less invasive all-ceramic restoration. With these superior properties, it is possible to secure a strong frame, even with a thickness of 0.5 mm, which enables porcelain faced prosthetic restoration by providing the frame design.

On the contrary, the results of the present study were in disagreement with those obtained by Fischer and Stawarczyk [69]. They found similar fracture resistance between NANOZR and Y-TZP. This difference in fracture resistance values could be attributed to the difference in the thickness of zirconia frameworks used and the veneering layer. Zirconia frameworks were constructed with an overall thickness of 0.7 mm, but framework thickness of 0.3 mm for NANOZR and 0.5 mm for Y-TZP were used in the current study. Moreover, veneering ceramic Cerabien ZR was used in their study while Vita VM9 was used in the current study.

Additionally, it was found that, there was a negative (inverse) correlation between fracture resistance and marginal gap, which agrees with Abd El Aziz et al. [70], who stated that the production method and the material composition influenced the quality of the crown margin as well as the load at fracture. Consequently, the increase in the marginal gap is regarded as a weakness spot that contributes to the loss of fracture resistance which might be attributed to the size of the nanoparticles.

Thus, the null hypothesis was disproved in light of the study's findings. After thermomechanical aging, NANOZR outperformed Y-TZP in both fracture resistance and marginal adaptation, underscoring the influence of its nanostructured composition on clinical performance. Nevertheless, several experimental limitations must be considered when interpreting these outcomes, including differences in framework thickness between groups, the use of model dies instead of natural teeth, the lack of internal gap assessment, the restriction to a single cement type and molar crown design, and the absence of preaging fracture resistance controls may have influenced the results [71]. Hence, future investigations using diverse preparation geometries and prosthetic designs are warranted to validate these findings under broader clinical conditions.

5. Conclusions

In conclusion, NANOZR restorations demonstrated superior marginal adaptation compared to Y-TZP restorations after thermocycling, although both materials exhibited an increase in marginal gap following the aging process. Furthermore, NANOZR showed significantly higher fracture resistance than Y-TZP after thermomechanical aging. A negative correlation was also observed between fracture resistance and marginal gap, suggesting that greater marginal discrepancies are associated with reduced fracture strength.

Data Availability Statement

Upon request, the corresponding author will provide the data used to support the results of the research.

Disclosure

This manuscript is part of a thesis that was previously published [72].

Conflicts of Interest

The authors declare no conflicts of interest.

Funding

The authors received no specific funding for this work.

References

- [1] S. M. Alqahtani, S. Chaturvedi, M. K. Addas, et al., "Internal and Marginal Fit of Digitally Fabricated All-Ceramic Crowns With Auxiliary Retentive Features on Short Clinical Abutments: A Micro-CT Study," *PeerJ* 13 (2025): e19813.
- [2] N. A. Fernandes, Z. I. Vally, and L. M. Sykes, "The Longevity of Restorations-A Literature Review," *South African Dent Journal* 70, no. 9 (2015): 410–413.
- [3] G. W. Jang, H. S. Kim, H. C. Choe, and M. K. Son, "Fracture Strength and Mechanism of Dental Ceramic Crown With Zirconia Thickness," *Procedia Engineering* 10 (2011): 1556–1560.
- [4] E. D. Rekow, N. Silva, P. G. Coelho, Y. Zhang, P. Guess, and V. P. Thompson, "Performance of Dental Ceramics: Challenges for Improvements," *Journal of Dental Research* 90, no. 8 (2011): 937–952.
- [5] F. Zhang, K. Vanmeensel, M. Inokoshi, et al., "Critical Influence of Alumina Content on the Low Temperature Degradation of 2–3 mol% Yttria-Stabilized TZP for Dental Restorations," *Journal of the European Ceramic Society* 35, no. 2 (2015): 741–750.
- [6] Y. Okuda, M. Noda, H. Kono, M. Miyamoto, H. Sato, and S. Ban, "Radio-Opacity of Core Materials for All-Ceramic Restorations," *Dental Materials Journal* 29, no. 1 (2010): 35–40.
- [7] S. Tanaka, M. Takaba, Y. Ishiura, E. Kamimura, and K. Baba, "A 3-Year Follow-up of Ceria-Stabilized Zirconia/Alumina Nanocomposite (Ce-TZP/A) Frameworks for Fixed Dental Prostheses," *Journal of Prosthodontic Research* 59, no. 1 (2015): 55–61.
- [8] Y. Kawai, M. Uo, Y. Wang, S. Kono, S. Ohnuki, and F. Watari, "Phase Transformation of Zirconia Ceramics by Hydrothermal Degradation," *Dental Materials Journal* 30, no. 3 (2011): 286–292.
- [9] H. T. Kim, J. S. Han, J. H. Yang, J. B. Lee, and S. H. Kim, "The Effect of Low Temperature Aging on the Mechanical Property & Phase Stability of Y-TZP Ceramics," *The Journal of Advanced Prosthodontics* 1, no. 3 (2009): 113–117.
- [10] M. Nishizaki, S. Komasa, Y. Taguchi, H. Nishizaki, and J. Okazaki, "Bioactivity of NANOZR Induced by Alkali Treatment," *International Journal of Molecular Sciences* 18, no. 4 (2017): 780.
- [11] R. A. Bapat, H. J. Yang, T. V. Chaubal, et al., "Review on Synthesis, Properties and Multifarious Therapeutic Applications of Nanostructured Zirconia in Dentistry," *RSC Advances* 12, no. 20 (2022): 12773–12793.
- [12] S. Ban, H. Sato, Y. Suehiro, H. Nakanishi, and M. Nawa, "Biaxial Flexure Strength and Low Temperature Degradation of Ce-TZP/Al₂O₃ Nanocomposite and Y-TZP as Dental

- Restoratives," *Journal of Biomedical Materials Research Part B: Applied Biomaterials* 87B, no. 2 (2008): 492–498.
- [13] H. Sato, K. Yamada, G. Pezzotti, M. Nawa, and S. Ban, "Mechanical Properties of Dental Zirconia Ceramics Changed With Sandblasting and Heat Treatment," *Dental Materials Journal* 27, no. 3 (2008): 408–414.
- [14] M. Bankođlu Güngör, A. Dođan, B. Turhan Bal, and S. Nemly, "Evaluation of Marginal and Internal Adaptations of Posterior All-Ceramic Crowns Fabricated With Chair-Side CAD/CAM System: An In Vitro Study," *Acta Odontologica Turcica* 35 (2018).
- [15] F. Beuer, B. Steff, M. Naumann, and J. A. Sorensen, "Load-Bearing Capacity of All-Ceramic Three-Unit Fixed Partial Dentures With Different Computer-Aided Design (CAD)/Computer-Aided Manufacturing (CAM) Fabricated Framework Materials," *European Journal of Oral Sciences* 116, no. 4 (2008): 381–386.
- [16] C. J. Goodacre, W. V. Campagni, and S. A. Aquilino, "Tooth Preparations for Complete Crowns: An art Form Based on Scientific Principles," *The Journal of Prosthetic Dentistry* 85, no. 4 (2001): 363–376.
- [17] M. R. Alammari, M. H. Abdelnabi, and A. A. Swelem, "Effect of Total Occlusal Convergence on Fit and Fracture Resistance of Zirconia-Reinforced Lithium Silicate Crowns," *Clinical, Cosmetic and Investigational Dentistry* 11 (2018): 1–8.
- [18] M. Bankođlu Güngör and S. Karakoca Nemli, "Fracture Resistance of CAD-CAM Monolithic Ceramic and Veneered Zirconia Molar Crowns After Aging in a Mastication Simulator," *The Journal of Prosthetic Dentistry* 119, no. 3 (2018): 473–480.
- [19] F. Beuer, D. Edelhoff, W. Gernet, and M. Naumann, "Effect of Preparation Angles on the Precision of Zirconia Crown Copings Fabricated by CAD/CAM System," *Dental Materials Journal* 27, no. 6 (2008): 814–820.
- [20] E. A. Naumova, S. Schneider, W. H. Arnold, and A. Piwowarczyk, "Wear Behavior of Ceramic CAD/CAM Crowns and Natural Antagonists," *Materials* 10, no. 3 (2017): 244.
- [21] Y. E. Ezzat and M. A. Al-Rafee, "Effect of Veneering Material and Technique on the Fracture Resistance of Porcelain-Veneered Zirconia Crowns," *Saudi Journal of Oral Sciences* 7, no. 1 (2020): 11–17.
- [22] J. Kim, Y. Hong, Y. Kang, J. Kim, and J. Shim, "Accuracy of Scanned Stock Abutments Using Different Intraoral Scanners: An In Vitro Study," *Journal of Prosthodontics* 28, no. 7 (2019): 797–803.
- [23] W.-S. Lee, D.-H. Lee, and K.-B. Lee, "Evaluation of Internal Fit of Interim Crown Fabricated With CAD/CAM Milling and 3D Printing System," *The Journal of Advanced Prosthodontics* 9, no. 4 (2017): 265–270.
- [24] F. Ferrini, G. Sannino, C. Chiola, P. Capparé, G. Gastaldi, and E. F. Gherlone, "Influence of Intra-Oral Scanner (I.O.S.) on The Marginal Accuracy of CAD/CAM Single Crowns," *International Journal of Environmental Research and Public Health* 16, no. 4 (2019): 544.
- [25] K. Haggag, M. Abbas, and H. Ramadan, "Effect of Thermo-Mechanical Aging on The Marginal Fit of Two Types of Monolithic Zirconia Crowns With Two Finish Line Designs," *Al-Azhar Dental Journal for Girls* 5, no. 1 (2018): 121–128.
- [26] L. Elbanna, E. Essam, M. AL-Yasaky, and H. Katamish, "Effect of Different CAD/CAM Techniques on Marginal Accuracy, Color Matching and Retention of Cemented Versus Screw Retained Implant-Supported Crowns," *Al-Azhar Dental Journal for Girls* 6, no. 4 (2019): 493–506.
- [27] T. Sawada, *Effect of a Novel Framework Design in Ceria-Stabilized Zirconia/Alumina Nanocomposite (Ce-TZP/A)-Based All-Ceramic Crowns* (Universität Tübingen, 2016).
- [28] M. Zahran, O. El-Mowafy, L. Tam, P. A. Watson, and Y. Finer, "Fracture Strength and Fatigue Resistance of All-Ceramic Molar Crowns Manufactured with CAD/CAM Technology," *Journal of Prosthodontics* 17, no. 5 (2008): 370–377.
- [29] R. Sorrentino, C. Triulzio, M. G. Tricarico, G. Bonadeo, E. F. Gherlone, and M. Ferrari, "In Vitro Analysis of the Fracture Resistance of CAD–CAM Monolithic Zirconia Molar Crowns With Different Occlusal Thickness," *Journal of the Mechanical Behavior of Biomedical Materials* 61 (2016): 328–333.
- [30] M. Ferrari, A. Giovannetti, M. Carrabba, et al., "Fracture Resistance of Three Porcelain-Layered CAD/CAM Zirconia Frame Designs," *Dental Materials* 30, no. 7 (2014): e163–e168.
- [31] G. E. Hamza, H. N. Salem, and M. A. Samman, "Evaluation of Two-Body Wear Rate and Roughness of Polyetheretherketone and Zirconia Opposing Enamel Structure: An in-Vitro Study," *Journal of The Arab Society for Medical Research* 14, no. 2 (2019): 73–81.
- [32] N. Nawafleh, M. Hatamleh, S. Elshiyab, and F. Mack, "Lithium Disilicate Restorations Fatigue Testing Parameters: A Systematic Review," *Journal of Prosthodontics* 25, no. 2 (2016): 116–126.
- [33] J. J. E. Choi, C. E. Uy, P. Plaksina, R. S. Ramani, R. Ganjigatti, and J. N. Waddell, "Bond Strength of Denture Teeth to Heat-Cured, CAD/CAM and 3D Printed Denture Acrylics," *Journal of Prosthodontics* 29, no. 5 (2020): 415–421.
- [34] M. A. Yousry, S. A. Hussein, and F. H. Al Abbassy, "Evaluation of Shear Bond Strength of High-Performance Polymers to Its Resin Veneering and to Dentin (In Vitro Study)," *Alexandria Dental Journal* 43, no. 2 (2018): 62–68.
- [35] T. Abdel-Azim, K. Rogers, E. Elathamna, A. Zandinejad, M. Metz, and D. Morton, "Comparison of the Marginal Fit of Lithium Disilicate Crowns Fabricated With CAD/CAM Technology by Using Conventional Impressions and Two Intraoral Digital Scanners," *The Journal of Prosthetic Dentistry* 114, no. 4 (2015): 554–559.
- [36] R. A. El-Dessouky, M. M. Salama, M. A. Shakal, and A. M. Korsel, "Marginal Adaptation of CAD/CAM Zirconia-Based Crown During Fabrication Steps," *Tanta Dental Journal* 12, no. 2 (2015): 81–88.
- [37] K. Torabi, M. Vojdani, R. Giti, M. Taghva, and S. Pardis, "The Effect of Various Veneering Techniques on the Marginal Fit of Zirconia Copings," *The Journal of Advanced Prosthodontics* 7, no. 3 (2015): 233–239.
- [38] Y. Tsuyuki, T. Sato, S. Nomoto, et al., "Effect of Occlusal Groove on Abutment, Crown Thickness, and Cement-Type on Fracture Load of Monolithic Zirconia Crowns," *Dental Materials Journal* 37, no. 5 (2018): 843–850.
- [39] K. Sieper, S. Wille, and M. Kern, "Fracture Strength of Lithium Disilicate Crowns Compared to Polymer-Infiltrated Ceramic-Network and Zirconia Reinforced Lithium Silicate Crowns," *Journal of the Mechanical Behavior of Biomedical Materials* 74 (2017): 342–348.
- [40] Y. El Makawi and N. Khattab, "In Vitro Comparative Analysis of Fracture Resistance of Lithium Disilicate Endocrown and Prefabricated Zirconium Crown in Pulpotomized Primary Molars," *Open Access Macedonian Journal of Medical Sciences* 7, no. 23 (2019): 4094–4100.

